ELSEVIER

Journal of Luminescence 86 (2000) 107–116

JOURNAL OF LUMINESCENCE

www.elsevier.com/locate/jlumin

Picosecond fluorescence decay and exciton dynamics in a new far-red molecular J-aggregate system

Mikhail Drobizhev[a,b,*], Christophe Sigel[a], Aleksander Rebane[a]

[a]*Department of Physics, Montana State University, Bozeman, MT 59717-3840, USA*
[b]*Permanent address: Lebedev Physics Institute, Leninsky Prospekt 53, 117924 Moscow, Russia*

Received 17 June 1999; received in revised form 7 October 1999; accepted 7 October 1999

Abstract

We present and characterize a new J-aggregate-type nanostructure formed by self-assembling of 3,3′-diethylthiadicarbocyanine iodide molecules in a solution. We measure picosecond kinetics of fluorescence from the lowest exciton band, lying in the far-red wavelength range around 810–830 nm. At temperatures 4–300 K we observe a non-exponential fluorescence decay and show that this is a result of exciton–exciton annihilation in a small exciton domain regime. We also measure the temperature dependence of single-exciton radiative lifetime and give a consistent description of it in terms of a self-trapping of exciton in a discrete one-dimensional chain. © 2000 Elsevier Science B.V. All rights reserved.

Keywords: J-aggregates; Infrared absorption; Exciton relaxation dynamics; Time-resolved fluorescence; Temperature dependence

1. Introduction

J-aggregates [1,2] are self-assembling low-dimensional nanostructures with unusual photophysical and optical properties. The aggregates are formed by binding together of a large number ($N \gtrsim 10$–100) identical molecules either by electrostatic or van der Waals interaction. In isotropic solutions, cyanine dye molecules organize themselves spontaneously into long one-dimensional (1D) chains [3,4], or they can assemble on a surface in the form of two-dimensional (2D) brickstone-like structures [5]. Because of resonant dipole–dipole interaction between adjacent molecules and because of translational symmetry of the system, absorption of a photon produces a coherent delocalized excitation or exciton. As early as in 1938, Franck and Teller adopted a picture of Frenkel-type excitons in J-aggregates, which allowed them to explain the exceptionally narrow spectral width of the absorption, as well as the shift of the resonance towards longer wavelengths with respect to the absorption maximum of the monomer [6].

An exciton involves a collective oscillation of N adjacent dipoles in a chain or in a lattice of molecules, leading to an N-fold enhancement of the transition oscillator strength and a corresponding increase of the probability of absorption and emission of light. In J-aggregates the large value of the oscillator strength manifests itself as a drastic shortening of spontaneous radiative decay time [7,8]. The lifetime of the exciton can be further reduced by an exciton-exciton annihilation process, resulting in a picosecond- or even sub-picosecond relaxation rate. On the other hand, large oscillator

* Corresponding author.

0022-2313/00/$ - see front matter © 2000 Elsevier Science B.V. All rights reserved.
PII: S0022-2313(99)00201-X

strength also provides for an increased value of resonant non-linear $\chi^{(3)}$-coefficient, which typically scales as N^2 [9] and can amount in large aggregates to 10^{-7}–10^{-5} esu [10]. This unique combination of high optical non-linearity with a very fast relaxation rate makes J-aggregates attractive as a new material for ultrafast optical switching and signal processing [11]. Very recently it was proposed to apply J-aggregates to implement a "polariton laser", which would make use of an efficient Rabi splitting of the resonant exciton absorption band in a microcavity [12]. In addition, molecular aggregates find use in photography as photosensitizers [13] and are also studied as a model for harvesting and conversion of solar energy [14].

For optical switching and signal processing applications it is very important that the resonance enhancement of the non-linear susceptibility occurs at a wavelength accessible to common diode lasers, $\lambda > 800$ nm. Most preferably, the working wavelength should be at the fiber communications range, $\lambda = 1500$–1600 nm. The wavelength of the J-band depends on the transition frequency of the parent monomer as well as on the value of the excitonic splitting. In carbocyanine dyes it is known that the frequency of the monomer transition decreases with increasing length of the conjugated polymethine chain. Furthermore, the stronger is the resonance coupling in the aggregate, the more red-shifted is the lowest excitonic transition, responsible for the J-absorption band.

The majority of J-aggregates studied so far show an exciton absorption band in the range $\lambda_m = 570$–700 nm. Pseudoisocyanine (PIC) aggregates is the most extensively studied system with $\lambda_m = 570$–580 nm [3,7,8,10,15,16]. In different benzimidazolocarbocyanines $\lambda_m = 580$–604 nm [17–19] and thiacarbocyanines $\lambda_m = 610$–700 nm [4,12,20–26] have been observed. So far, there are only a few reports on J-aggregate absorption bands in far-red range, with $\lambda_m = 725$ nm [27] and $\lambda_m = 800$ nm [28]. To our knowledge, no studies of time-resolved exciton relaxation dynamics or corresponding non-linear response characteristics have been performed in the wavelength region $\lambda_m > 700$ nm. Therefore, it is an important task to search for new aggregate systems with longer wavelength absorption bands, suitable for diode lasers.

An equally important goal is to understand the physical mechanism of the enhancement of the optical oscillator strength and its relation to the structure of the aggregates. In spite of rather extensive studies, the nature of relaxed excited states in J-aggregates is not yet completely understood. Wiersma and co-workers have found that the fluorescence radiative lifetime of PIC J-aggregates in isotropic solution decreases by a factor of 20 if the temperature is lowered from 140 to 30 K [7,8]. This rather intriguing fact has been explained qualitatively in terms of an enhancement of the optical oscillator strength in proportion to the coherence length of the exciton, which, in turn, is assumed to increase with a decreasing temperature, because of fewer exciton–phonon scattering events [7]. For quantitative description, however, the one-dimensional exciton–phonon scattering model, stated in Ref. [3] for the same system [7,8], appeared to be unsatisfactory and the authors [18,29] had to resort to more sophisticated models with higher dimensionality.

In the present paper we describe the preparation and analyze the optical properties of a new J-aggregate system, which shows absorption and emission in far-red region of the spectrum. Depending on temperature, these new aggregates present a J-band with a maximum at $\lambda_m = 806$–825 nm. We apply picosecond time-resolved fluorescence measurements to study the dynamics of exciton relaxation as a function of temperature. To explain the observed dependencies, we apply a model, which takes into account an inherent instability of a linear chain of molecules with respect to a phonon-induced distortion. This instability leads to the fact that excitons can be efficiently self-trapped without needing to overcome an energy barrier. The effect of barrier-less self-trapping was used earlier to explain the spectral features of fluorescence of different J-aggregates [20–22]. Here we apply this approach to explain the behavior of excitonic radiative lifetime.

2. Experimental

For sample preparation we used 3,3'-diethylthiadicarbocyanine iodide (DTDCI) purchased

from Aldrich. The dye was dissolved in bi-distilled water at a concentration of 4×10^{-3} M upon heating to 60°C. 0.1 M concentration of KCl (Aldrich) was added to the hot dye solution. After cooling down to room temperature, a characteristic J-band appeared in the red side of the spectrum (Fig. 1). Then, the solution was diluted by adding 50% glycerol (Aldrich). The final concentrations of the dye and of the salt were 2×10^{-3} and 0.05 M, respectively. The addition of glycerol resulted in a decrease of the optical density of the J-band, but was necessary to obtain transparent samples upon freezing. For low-temperature studies, one drop of the solution was deposited between two glass plates separated by a 1-mm thick spacer ring. The sample was quickly inserted in liquid nitrogen and then transferred to an optical liquid helium cryostat. Absorption spectra were measured with a Perkin–Elmer Lambda 900 spectrophotometer. Fluorescence spectra were measured with Acton SpectraPro - 300i spectrograph coupled with CCD camera.

Fluorescence was excited at 755 nm in time-resolved measurements and at 775 nm in spectral measurements with a mode-locked Ti : sapphire laser Coherent Mira 900, pumped by Coherent Innova 200 Argon Ion laser. The excitation pulses had duration of 200 fs with 76 MHz repetition rate.

In time-resolved experiments, the optical density of the sample in the region of the J-band was below 0.15, which minimized fluorescence re-absorption

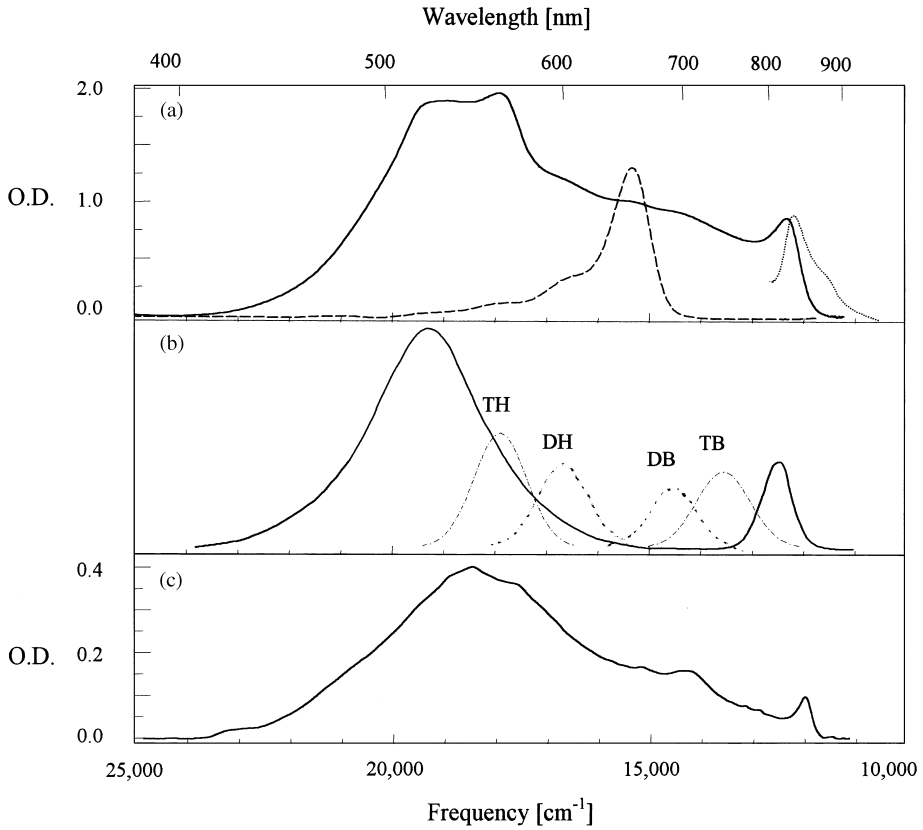

Fig. 1. (a) Room temperature absorption spectrum of freshly prepared aggregate solution in water with addition of KCl (solid curve) and DTDCI monomers in methanol (dashed curve). Normalized fluorescence spectrum of J-aggregates at room temperature (dotted curve). (b) Decomposition of the aggregate solution spectrum into constituent components: pure J-aggregates (solid curve), dimer H-band (DH), dimer B-band (DB), trimer H-band (TH) and trimer B-band (TB); Residual monomer absorption is not shown. (c) Absorption spectrum of the aggregates in water/glycerol solution at 77 K (c).

effects. In this case the Ti : sapphire laser beam was attenuated with neutral density filters and uniformly focused with a $f = 80$ mm lens onto a 1-mm diameter spot on the sample inside the cryostat. The measured photon flux on the sample was varied between 10^{11} and 10^{12} photons/(cm^2 pulse) by varying neutral density filters. The fluorescence signal was collected at 90° angle with an 1 : 1.7 relative aperture objective lens and was focused on the entrance slit of a Hamamatsu C5680-31 synchroscan streak camera. The fluorescence spectrum is almost resonant with the J-absorption, as shown below. Therefore, to avoid collecting excessive amount of scattered laser light, we used a set of IR filters. Residual transmitted laser light was removed from measured fluorescence decay curves by subtraction. The prompt response of the camera system was obtained by placing a scattering paper in the laser beam at the position of the sample. In our experiment, the half width (at 1/e of the peak intensity) of the prompt response was about 10 ps.

3. Results and discussion

The dashed line in Fig. 1(a) shows room temperature monomer absorption of DTDCI in methanol solution. The maximum of the $S_1 \leftarrow S_0$ band is at 15 380 cm^{-1} (650 nm). The solid line presents room temperature absorption of a freshly prepared aggregate sample. One can clearly identify a narrow red-shifted peak, characteristic to J-aggregates, which is accompanied by several other partially overlapping peaks at shorter wavelengths. Aggregate fluorescence spectrum (dotted line in Fig. 1(a)) also shows the pronounced J-band, which is shifted by 300 cm^{-1} to lower energies with respect to absorption maximum. The highest-energy component of the aggregate absorption spectrum (Fig. 1(b), solid line) can be well approximated with a Lorentzian, with a peak at 19 200 cm^{-1} (521 nm) and with 2800 cm^{-1} full-width at half-maximum. It was shown earlier [23] that J-aggregates formed of thiacarbocyanine dyes tend to have two molecules per unit cell, arranged in an oblique W-like geometry. In this case, one expects to observe in the absorption spectrum a set of two allowed transitions, corresponding to the two Davydov-split components of the exciton band. Based on this simple picture, we assign the 19 200 cm^{-1} peak to the upper Davydov component, frequently called H-band. The pronounced Lorentzian shape of the H-band indicates an almost homogeneous broadening due to very fast non-radiative relaxation to lower-lying band states, with a time constant, $\tau \sim 2$ fs. The energy band, appearing at 12 410 cm^{-1} (806 nm) belongs to the lower Davydov component of the J-aggregate, usually called J-band. Together, the J-band and the Lorentzian-approximated H-band form the absorption spectrum of the new J-aggregate system, shown as a solid curve in Fig. 1(b).

To analyze the origin of the other bands, we subtract from the spectrum Fig. 1(a) the pure J-aggregate spectrum, together with a residual monomer absorption at 15 380 cm^{-1}. The remaining absorption can be well described by a superposition of 4 Gaussian bands, shown as dashed curves in Fig. 1(b). In Ref. [30] the absorption and relaxation properties of dimers and trimers of DTDCI were studied. We use this data to assign the bands at 16 570 cm^{-1} (603 nm) and 17 800 cm^{-1} (564 nm) to H-component of the dimer- and trimer of DTDCI molecules, formed as an inevitable by-product of the aggregation process. Similarly, the bands at 14 400 cm^{-1} (694 nm) and 13 460 cm^{-1} (743 nm) can be assigned to the lower-energy transitions of the same dimer and trimer, which we call B-bands. An argument in support of this assignment is that the difference between the B-band energy and the monomer energy, ΔE_B, has a comparable value as the separation between the monomer and the corresponding H-bands, ΔE_H. Note, however, that if the splitting in the dimer spectrum is almost symmetrical ($\Delta E_H \approx 1200$ cm^{-1} vs. $\Delta E_B \approx 1000$ cm^{-1}), the splitting in the trimer spectrum is somewhat less symmetrical ($\Delta E_H \approx 2400$ cm^{-1} vs. $\Delta E_B \approx 1900$ cm^{-1}). This slight asymmetry is expected because of the difference, which exists in the strength of van der Waals interaction of adjacent molecules in the ground and excited states [31]. Comparable area under the dashed curves in Fig. 1(b) suggest that the corresponding transitions have similar oscillator strength. This indicates [31] that in the dimer and trimer, the individual dye molecules are

also arranged in an oblique geometry, as in the case of the larger J-aggregates.

In the aggregate spectrum, the H-band has a considerably higher transition probability than the J-band. By integrating the areas under the corresponding bands, we can estimate the ratio of the oscillator strengths to be $f_H/f_J \approx 15$. For W-shaped linear chain aggregates [31],

$$\frac{\nu_J}{\nu_H}\frac{f_H}{f_J} \approx \frac{M_H^2}{M_J^2} = \tan^2\alpha, \tag{1}$$

where $M_{H,J}$ and $\nu_{H,J}$ are the transition dipole moments and the transition frequencies of the H- and J-bands, respectively, and α is the angle between the molecule transition dipole moment vector and the axis of the aggregate chain. Knowing that the transition dipole of DTDCI molecule lies more or less in the direction of the polymethine backbone, we can estimate the tilt angle of the molecules in the chain to be, $\alpha \approx 70^\circ$.

From Fig. 1(b) we see that the splitting asymmetry of the J-aggregate ($\Delta E_H \approx 3800\,\mathrm{cm}^{-1}$ vs. $\Delta E_J \approx 3000\,\mathrm{cm}^{-1}$) is even higher than that in the trimer. Furthermore, the total excitonic bandwidth $2B = \Delta E_H + \Delta E_J \approx 6800\,\mathrm{cm}^{-1}$ is found to be extremely large as compared to other known J-aggregates in solutions. For example, this splitting is about twice as large as that measured for THIATS ($2B = 3150\,\mathrm{cm}^{-1}$), which is another thiacarbocyanine dye showing a distinct Davydov splitting [24]. In the case of the oblique spatial arrangement, the value of the total excitonic splitting can be expressed as [31]:

$$2B = 4\frac{N-1}{N}\frac{M^2}{R^3}(1+\cos^2\alpha), \tag{2}$$

where R is the distance between adjacent molecules and M is the monomer transition dipole moment. Thus, the splitting is proportional to the square of monomer transition dipole moment, where the latter value is related to the inverse radiative lifetime of the monomer transition

$$M^2 \propto \frac{1}{\nu^3 \tau_R^m}, \tag{3}$$

where ν is the transition frequency. The radiative lifetime for THIATS and DTDCI was measured to be 5 ns [24] and 3.4–4.2 ns [30,32], respectively. By inserting the values for the corresponding transition frequencies, $\nu_{THIATS} \approx 17\,900\,\mathrm{cm}^{-1}$ [24] and $\nu_{DTDCI} \approx 15\,400\,\mathrm{cm}^{-1}$, we obtain from (3)

$$\frac{M_{DTDCI}^2}{M_{THIATS}^2} = 1.9\text{–}2.3. \tag{4}$$

This value corresponds well with the observed difference of excitonic splitting in two systems, which justifies, in part, the assumption that the intermolecular distances are approximately the same for DTDCI and THIATS J-aggregates (assuming that $N \gg 1$, $\cos^2\alpha < 0.1$ and R is the same for both aggregates). We can conclude that the two-fold enhancement of the excitonic splitting in DTDCI J-aggregates is mostly due to longer wavelength of the monomer transition. It follows that in order to push the J-band absorption even further towards the infrared wavelengths, one may need to consider aggregates assembled from similar kind of polymethine dye molecules, but with a longer conjugated chain.

Fig. 1(c) shows the absorption spectrum of the aggregates at 77 K. We observe almost the same set of bands as described above. The ratio of the Davydov splitting components is now, $f_H/f_J \approx 45$, thus yielding a slightly larger tilt angle, $\alpha \approx 80^\circ$. J-band appears now at 825 nm, which means that the full splitting is even higher at low temperature, $2B = 7060\,\mathrm{cm}^{-1}$. These observations can be explained due to a shortening of the intermolecular distances and an increase of an effective number of coherently coupled molecules.

Fig. 2 shows the fluorescence decay measured at different temperatures, $T = 5$, 50 and 130 K. The excitation intensity was kept constant and equal to 10^{11} photons/cm^{2}s in order to avoid saturation effects. The decay contains a distinct fast component with a decay constant less than 100 ps. At delay times larger than 100 ps the decay behavior changes over into a single exponential dependence. A significant observation is that the long exponential decay is faster at lower temperature and slower at higher temperature. Such unusual temperature dependence has been observed earlier for other J-aggregate systems [7,17]. It should be noted, however, that not all J-aggregates show this kind of

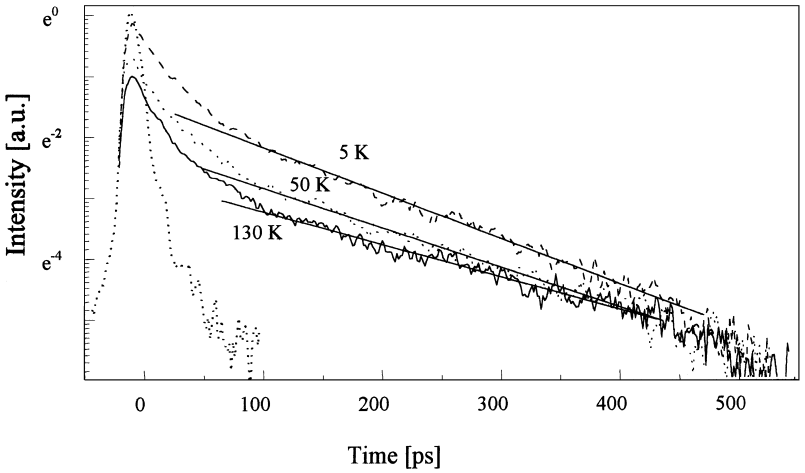

Fig. 2. Fluorescence decay kinetics measured at 5 (dashed), 50 (dotted), and 130 K (solid). Straight lines are exponential approximations to fit the slow decay component at times $t > 100$ ps. Response function to laser excitation pulses is shown for comparison.

behavior, and in some cases decay slows down at low temperatures [4,18,19,26].

Fig. 3 presents results of a detailed measurement of the variation of the fast and the slow decay constants as well as of the integrated fluorescence intensity in the temperature range $T = 4$–150 K. The decay constants were obtained by applying a standard two-exponential decomposition technique. From Fig. 3 (a) we see that as the temperature decreases from 150 to 4 K, the slow component changes from $\tau \approx 170$ to $\tau \approx 120$ ps, whereas the fast component $\tau \approx 20$ ps does not depend on temperature in any significant manner. The overall integrated fluorescence intensity, F_{int}, decreases with increasing temperature, as shown in Fig. 3 (b). In the same way as in a number of previous investigations [8,17–19], we can attribute the decrease of F_{int} with increasing temperature to an accelerated non-radiative relaxation rate, which competes with the radiative process.

In order to correctly interpret the fast fluorescence component, we need first to exclude a simple possibility of fluorescence originating from DTDCI trimers, which are known to have a fast fluorescence decay (20–50 ps at room temperature) [30]. Because in our case the absorption band of trimers overlaps the absorption of J-aggregates, a straightforward spectral discrimination between these two is difficult. Instead, we notice that the relative contribution of the fast and slow components to the integrated fluorescence intensity remains constant with temperature. Such behavior is not expected, if the fluorescence would be due to two or more

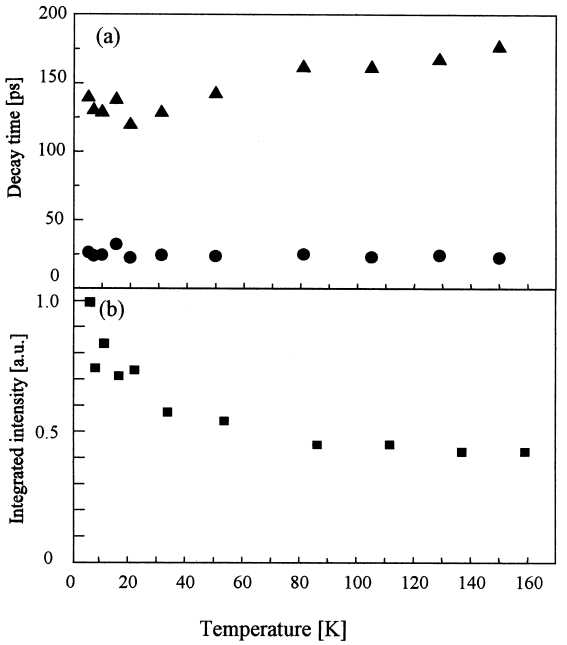

Fig. 3. (a) Temperature dependence of the fast (circles) and the slow (triangles) decay times. (b) Temperature dependence of the-integrated fluorescence intensity.

different species with presumably different fluorescence quenching mechanisms. This fact leads us to believe that both the fast and the slow decay originate from the same aggregate specie.

The physically relevant explanation of the fast decay consists in exciton–exciton annihilation [15,16,25]. Our present analysis is based on a theory [33], which takes into account the annihilation in restricted domains. According to this theory, the annihilation-driven fluorescence decay can be approximated by a series of exponents

$$F(t) \approx A_0(Z,r)\mathrm{e}^{-Kt} + A_1(Z,r)\mathrm{e}^{-(r+1)\gamma t} + A_2(Z,r)\mathrm{e}^{-0.75(r+2)\gamma t} + \cdots, \quad (5)$$

where K is the mono-excitonic decay rate and γ is the annihilation rate for a pair of excitons. Coefficients $A_i (i = 0, 1, 2, \ldots)$ are functions of two parameters: $r = 2K/\gamma$ and Z, where the last is the average number of acts of absorbed photons per domain, which in turn is proportional to the excitation intensity. The first term in the series corresponds to the intensity-independent mono-excitonic decay process with a single exponential constant, K, which is, in general, a temperature-dependent quantity. The next terms express the contribution from exciton–exciton annihilation. This process is not a single exponential decay and its average rate may depend on the excitation intensity, temperature as well as on the size of the restricted domain.

Depending on the domain size, one can deduce two limiting cases. If the domains are much smaller than the diffusion length of the excitons, then the annihilation rate has a larger value than the mono-excitonic decay, i.e., $r \ll 1$. In this case, the fluorescence kinetics becomes mono-excitonic after a short time, $t < \tau$, where $\tau = 1/K$. In the opposite case of large domains, the annihilation process lasts longer ($r \gg 1$), which means that the mono-excitonic decay recovers only after $t > 2\tau$ [25,33].

Fig. 2 shows that the fast decay lasts only a relatively short time, $t \approx 0.7\tau$, after which the curves become mono-exponential. Secondly, since we observe that the fast component does not depend on temperature, the exponential factors, $(r + 1)\gamma$ and $(r + 2)\gamma$ in the above formula should not depend on temperature. This is possible if $K \ll \gamma$, and γ is independent of temperature. Note that if $r \gg 1$, then the annihilation exponential factors will be proportional to K. This means that the fast decay should be varying with temperature, which our data do not show. Thus, we can conclude that for our new system, $r < 1$ and γ do not depend on temperature.

Our next step is to evaluate the oscillator strength of the exciton transition. For this we first need to find the relative radiative lifetime $\tau_R = 1/K_R$, where K_R is the radiative rate. τ_R is obtained by dividing the observed decay constant τ over the relative quantum yield. In the small domain limit, the theory [33] gives the following expression dependence for fluorescence quantum yield in the case of annihilation:

$$\Phi = \left(\frac{1 - \mathrm{e}^{-Z}}{Z}\right)\Phi_0, \quad (6)$$

where $\Phi_0 = K_R/K$ is the quantum yield in the absence of annihilation. As far as we are using the same excitation intensity at all temperatures, we may consider the function enclosed in the brackets on the right-hand side of Eq. (6) as independent of temperature. Φ is proportional to the time-integrated fluorescence intensity, F_{int}, see Fig. 3b.

With these assumptions, we can estimate the relative radiative lifetime as, $\tau_R \sim \tau/F_{int}$. Fig. 4 shows τ_R plotted as a function of temperature. One can see that initially the value of τ_R rises in the 5–80 K range and then saturates at higher temperatures. A nearly exponential increase of τ with temperature has been observed earlier for PIC J-aggregates [8]. A more smooth dependence has been found for J-aggregates of substituted benzimidocarbocynine (BIC) [18]. In both cases, some kind of saturation behavior was also present at $T > 130$ K.

Dashed curve in Fig. 4 shows our attempt to fit the data with a regular dependence, $\tau_R \propto T^{1/2}$ [34], following from a standard rigid one-dimensional chain model, and assuming an equilibrium thermal population of the band excitons. An obvious discrepancy between this theory and our data forces us to search for a better theoretical description. Our approach is to consider a soft one-dimensional chain, which allows for a change of local symmetry of the lattice as a result of electron–phonon

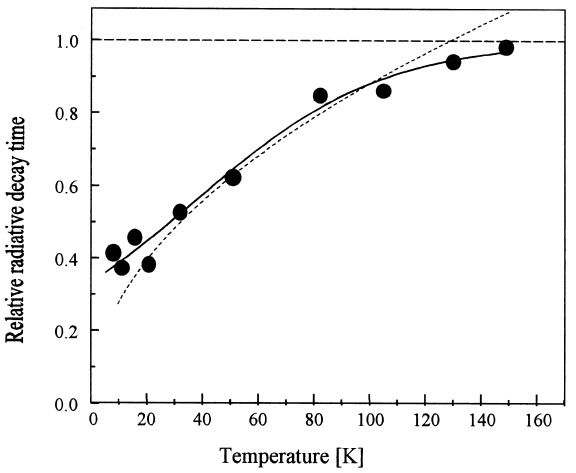

Fig. 4. Relative radiative lifetime, obtained as the ratio of the monoexcitonic decay time and integrated intensity of fluorescence. The dashed curve is a fit obtained from square root law; the solid curve is obtained from fitting according to Eqs. (8) and (9). The dashed horizontal line corresponds to a $T \to \infty$ limit of the radiative time.

relaxation. It was shown for the first time by Rashba [35] that in 1D chain a free exciton state can spontaneously transform into a self-trapped exciton state. A self-trapped state is associated with a well-defined local distortion of the lattice, where the latter can be regarded as some kind of correlated disorder in positions of molecules. Depending on the strength of coupling between exciton and phonons, the self-trapped state can be either strictly localized on one molecule or it can be spread out over several molecules.

The theory of self-trapped excitons or solitons in a one-dimensional chain has been successfully applied to explain small Stokes shift, temperature broadening of fluorescence bands and other characteristic features of J-aggregates [20–22]. Here we apply this approach to explain the temperature dependence of τ_R. It has been shown [36] that if the number of molecules bound in the soliton state is large, $N_b \gg 1$ (the so-called continuum approximation), then for a resting soliton-like state

$$\tau_R \propto \frac{\tau_R^m}{N_b} \propto \tau_R^m g, \tag{7}$$

where τ_R^m is the radiative lifetime of monomer and $g = G/B$ is a dimensionless exciton–phonon coupling parameter, where G is the energy of lattice relaxation for an exciton trapped on a single site. In continuum approximation one can show [37] that because of the decrease of resonance coupling energy B (or, equivalently, increase of effective mass of a particle), at sufficiently high temperatures, $kT > \hbar\omega$, where ω is a characteristic phonon frequency, the temperature dependence of g has a form

$$g = A e^{CT}, \tag{8}$$

where A and C are constants, only weakly depending on temperature. Note that because of the inverse dependence of N_b on g, and because the last increases exponentially with T, at higher temperatures the continuum approximation ceases to work. An improved version of formula (7) can be found on the basis of discrete version of soliton theory [38]

$$\tau_R = \frac{\tau_R^m}{N_b} = \frac{\tau_R^m g(1 + g^2/32)}{16(1 + g^2/64)^{3/2}}. \tag{9}$$

For small values of g, Eq. (9) gives the same result as the continuum approximation (7), whereas at large g it gives, $\tau_R \approx \tau_R^m$. The latter relation is a direct consequence of the fact that the soliton is localized on a single molecule, rather than spread out over many molecules.

Solid line in Fig. 4 shows the best theoretical fit obtained from Eqs. (8) and (9). In particular, this theoretical model describes rather well the sharp increase of τ_R at low T, followed by a saturation at higher T.

Finally, we estimate the number N_b of molecules bound together in the self-trapped exciton state. We assume that at high temperatures $T > 200$ K there is just one molecule bound in the exciton, i.e., $N_b \to 1$. On the other hand, in the low-temperature limit, the value of τ_R decreases by a factor of 3, which, according to Eq. (9) gives, $N_b \geq 3$. Further experiments will be needed for a more accurate estimation of N_b at different temperatures. Note, for the sake of comparison, that the N_b values were estimated earlier for J-aggregates of other thiacarbocyanines, TDC, and THIATS to be 7 and 17,

respectively [20,22]. We can roughly estimate now the relative (compared to a free monomer) oscillator strength, f_J, for J-band fluorescence, according to

$$\frac{f_J}{f_m} = \frac{\nu_m^2}{\nu_J^2} \cos^2\alpha N_b. \quad (10)$$

Substituting for $\alpha = 80°$, $N_b = 3$, $\nu_m = 15380\ cm^{-1}$ and $\nu_J = 12100\ cm^{-1}$, we obtain $f_J/f_m \approx 0.1$.

Note that this relatively small oscillator strength value corresponds to a relaxed self-trapped state and can be attributed to a sufficiently strong exciton–phonon coupling present in this particular system.

We should emphasize that our description of temperature dependence of radiative lifetime is not necessarily the only true one. We have shown only that the model of one-dimensional self-trapping accounts for observed behavior. On the other hand, the model [29] taking into account Boltzmann population of the 2D band exciton states (with particular geometry of the unit cell) can also qualitatively describe our results. However, in the case of 2D (or 3D) model, one gets additional degrees of freedom for fitting experimental data, which are dictated by the geometry of the unit cell. Therefore, the result depends on a particular arrangement of molecules (cf. different types of dependences for 2D case in Ref. [18,29]). For example, simple square and cubic arrangements of 2D and 3D lattices with Boltzmann population give $\tau_R \sim T$ and $\tau_R \sim T^{3/2}$, respectively [18]. Neither of these dependences can describe our experimental data.

Furthermore, we would like to stress that the 1D self-trapping model (Eqs. (7)–(9)) also describes satisfactorily other earlier experimental results on J-aggregates [8,18].

In summary, we can suppose the following sequence of events to take place in the DTDCI J-aggregate after creation of the exciton (excitons) at low temperatures. First, self-trapping of an initially almost free exciton occurs in a few picoseconds or less [22]. Then, these localized excitons can migrate incoherently over a certain domain resulting in exciton–exciton annihilation, if the number of excitons is high enough. The final step of the relaxation could be a radiative or non-radiative decay of mono-excitons with a time of 100–200 ps.

4. Conclusions

We have presented a new J-aggregate system, whose long-wavelength excitonic absorption band lies in a technologically important far-red range of wavelengths $\lambda > 800$ nm. We have shown that the shift of the J-band towards longer wavelengths is caused mainly by lower frequency of the corresponding 3,3'-diethylthiadicarbocyanine iodide monomer transition, which increases by a factor of two the Davydov splitting between the low- and high-energy bands. This gives a useful guideline for the future of how to lower the energy of the excitonic resonance further towards optical communications wavelengths.

For the first time, we have investigated exciton dynamics in a far-red molecular J-aggregate in a broad range of temperatures 4–300 K. By measuring the picosecond kinetics of the fluorescence from the J-band, we have observed that the mono-excitonic fluorescence decay time, which is independent of illumination intensity, decreases from 170 ps at 150 K to 120 ps at 4 K. Exciton–exciton annihilation gives rise to a fast fluorescence component with a decay time about 20 ps, which remains constant in the above temperature range at constant photon flux. We explain this behavior by applying an improved theoretical description, which takes into account the self-trapping of excitons in one-dimensional chain as well as the finite size of the exciton domain.

We believe that self-assembling nanostructures such as J-aggregates will become useful for practical applications in future optical computing and communications technology and that our results have revealed new possibilities for producing such materials operating in far-red and infrared wavelength range.

Acknowledgements

We are grateful to Lee Spangler for generous loan of the streak camera. We thank O.P. Varnavsky

and I.G. Scheblykin for useful discussion. This work was supported by NSF grant ECS-9712342 and in part by AFOSR grant F49620-98-1-0157.

References

[1] E.E. Jelley, Nature (London) 138 (1936) 1009.
[2] G. Scheibe, Angew. Chem. 49 (1936) 563.
[3] H. Fidder, J. Terpstra, D.A. Wiersma, J. Chem. Phys. 94 (1991) 6895.
[4] H. Fidder, D.A. Wiersma, J. Phys. Chem. 97 (1993) 11603.
[5] D. Möbius, Adv. Mater. 7 (1995) 437.
[6] J. Franck, E. Teller, J. Chem. Phys. 6 (1938) 861.
[7] S. De Boer, D.A. Wiersma, Chem. Phys. Lett. 165 (1990) 45.
[8] H. Fidder, D.A. Wiersma, Phys. Stat. Sol. B 188 (1995) 285.
[9] F.C. Spano, S. Mukamel, J. Chem. Phys. 91 (1989) 683.
[10] V.L. Bogdanov, E.N. Viktorova, S.V. Kulya, A.S. Spiro, JETP Lett. 53 (1991) 105.
[11] E. Gaizauskas, K-H. Feller, R. Gadonas, Opt. Commun. 118 (1995) 360.
[12] D.G. Lidzey, D.D.C. Bradley, T. Virgili, A. Armitage, M.S. Skolnick, S. Walker, Phys. Rev. Lett. 82 (1999) 3316.
[13] T.H. James, (Ed.), The Theory of Photographic Process, 4th Edition, Macmillan, New York, 1977.
[14] C. Königstein, R. Bauer, Sol. Energy and Sol. Cells 31 (1994) 535.
[15] V. Sundström, T. Gillbro, R.A. Gadonas, A. Piskarskas, J. Chem. Phys. 89 (1988) 2754.
[16] P.J. Reid, D.A. Higgins, P.F. Barbara, J. Phys. Chem. 100 (1996) 3892.
[17] J. Moll, S. Daehne, J.R. Durrant, D.A. Wiersma, J. Chem. Phys. 102 (1995) 6362.
[18] V.F. Kamalov, I.A. Struganova, K. Yoshihara, J. Phys. Chem. 100 (1996) 8640.
[19] U. de Rossi, U. Stahl, S. Dähne, M. Lindrum, S.C.J. Meskers, H.P.J.M. Dekkers, J. Fluoresc. 7 (1997) 715.
[20] M.A. Drobizhev, M.N. Sapozhnikov, I.G. Shcheblykin, O.P. Varnavsky, M. Van der Auweraer, A.G. Vitukhnovsky, Pure Appl. Opt. 5 (1996) 569.
[21] M.A. Drobizhev, M.N. Sapozhnikov, I.G. Shcheblykin, O.P. Varnavsky, M. Van der Auweraer, A.G. Vitukhnovsky, Chem. Phys. 211 (1996) 455.
[22] M.A. Drobizhev, in: D.L. Wise, G.E. Wnek, D.J. Trantolo, T.M. Cooper, J.D. Gresser (Eds.), Photonic Polymer Systems, Marcel Dekker, New York, 1998, p. 295, Chapter 9.
[23] I.G. Shcheblykin, M.A. Drobizhev, O.P. Varnavsky, M. Van der Auweraer, A.G. Vitukhnovsky, Chem. Phys. Lett. 261 (1996) 181.
[24] I.G. Shcheblykin, O.P. Varnavsky, W. Verbouwe, S. De Backer, M. Van der Auweraer, A.G. Vitukhnovsky, Chem. Phys. Lett. 282 (1998) 250.
[25] I.G. Shcheblykin, O.P. Varnavsky, M.M. Bataiev, O. Sliusarenko, M. Van der Auweraer, A.G. Vitukhnovsky, Chem. Phys. Lett. 298 (1998) 341.
[26] K. Kemnitz, K. Yoshihara, T. Tani, J. Phys. Chem. 94 (1990) 3099.
[27] A. Nabetani, A. Tomioka, H. Tamaru, K. Miyano, J. Chem. Phys. 102 (1995) 5109.
[28] V. Tkachev, A. Tolmachev, L. Chernigov, Yu. Slominsky, Thin Solid Films 245 (1994) 191.
[29] E.O. Potma, D.A. Wiersma, J. Chem. Phys. 108 (1998) 4894.
[30] V. Sundström, T. Gillbro, J. Chem. Phys. 83 (1985) 2733.
[31] M. Kasha, in: B. di Bartolo (Ed.), Spectroscopy of the Excited State, Nato ASI Series. Series B, Physics, Vol. 12, Plenum Press, New York, 1976, p. 337.
[32] D.N. Dempster, T. Morrow, R. Rankin, G.F. Thompson, J. Chem. Soc. Faraday Trans. 2 (68) (1972) 1479.
[33] G. Paillotin, C.E. Swenberg, J. Breton, N.E. Geacintov, Biophys. J. 25 (1979) 513.
[34] V.A. Malyshev, J. Lumin. 55 (1993) 225.
[35] E.I. Rashba, in: E.I. Rashba, M.D. Sturge (Eds.), Excitons, North-Holland, Amsterdam, 1982, p. 543.
[36] A.S. Davydov, A.A. Eremko, Ukr. Fiz. Zh. 22 (6) (1977) 881–893.
[37] D.W. Brown, Z. Ivić, Phys. Rev. B 40 (1989) 9876.
[38] V.A. Kuprievich, Physica D 14 (1985) 395.